

Starshade Design for Occulter Based Exoplanet Missions

Mark W. Thomson¹, P. Douglas Lisman¹, Richard Helms¹, Phil Walkemeyer¹,
Andrew Kissil¹, Otto Polanco¹, Siu-Chun Lee²,

¹Jet Propulsion Laboratory, California Institute of Technology, Pasadena, CA, 91109 USA

²Applied Sciences Laboratory, Baldwin Park, CA 91706 USA

ABSTRACT

We present a lightweight starshade design that delivers the requisite profile figure accuracy with a compact stowed volume that permits launching both the occulter system (starshade and spacecraft) and a 1 to 2m-class telescope system on a single existing launch vehicle. Optimal figure stability is achieved with a very stiff and mass-efficient deployable structure design that has a novel configuration. The reference design is matched to a 1.1m telescope and consists of a 15m diameter inner disc and 24 flower-like petals with 7.5m length. The total tip-to-tip diameter of 30m provides an inner working angle of 75 mas. The design is scalable to accommodate larger telescopes and several options have been assessed. A proof of concept petal is now in production at JPL for deployment demonstrations and as a testbed for developing additional elements of the design. Future plans include developing breadboard and prototype hardware of increasing fidelity for use in demonstrating critical performance capabilities such as deployed optical edge profile figure tolerances and stability thereof.

Keywords: Exoplanet, occulter, starshade

1. INTRODUCTION

Recent mission concept studies, including THEIA¹ and New Worlds Observer², establish the viability of free-flying occulter for finding and characterizing earth-like exoplanets. These are large flagship missions with 4m telescopes that also perform a robust observing program for general astrophysics. Current efforts focus on establishing more affordable occulter missions that might be fundable in the near future, while still achieving a large fraction of the exoplanet science objectives. Options currently under study include operating an occulter with JWST and the Occulting Ozone Observatory (O₃)³ with telescope apertures between 1 and 2m.

The starshade design presented here and illustrated in Figure 1 is matched to the O₃ mission with a 1.1m telescope, but it is scalable to include all options currently under consideration due to its stowed volumetric efficiency. It provides a 75 mas inner working angle (IWA) with a 30m tip-to-tip diameter and a separation distance between occulter and telescope of about 40,000 km. It consists of a 15m diameter inner disc and 24 flower-like petals with 7.5m length. An alternate design for a 2m telescope with a slightly relaxed IWA of 90 mas requires only a modest increase in the overall diameter to 34m. The inner disc of this design is 21m and the petals are actually shorter with a length of 6.5m.

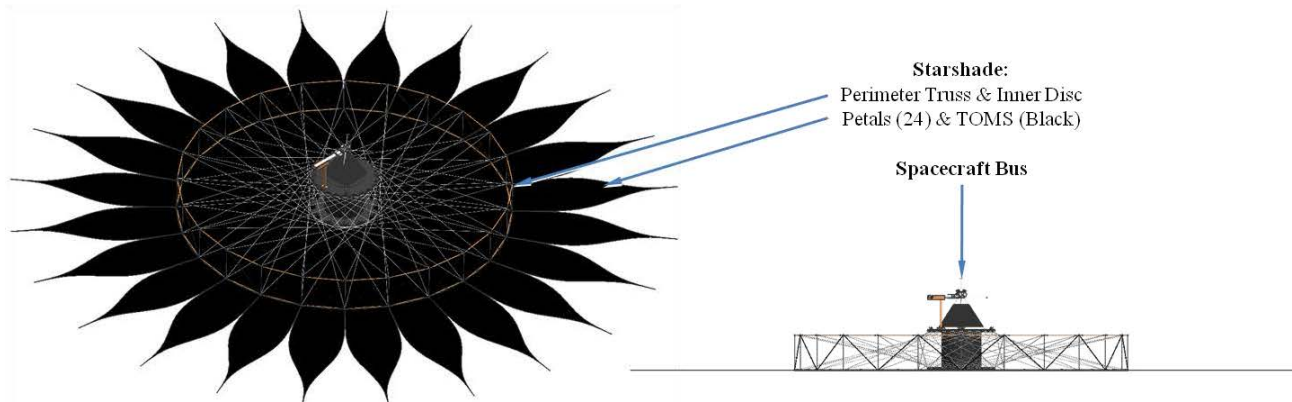


Figure 1. O₃ occulting spacecraft concept with 30m diameter deployable starshade

A deployable perimeter truss is used to form the inner disc and to provide a very stiff and stable interface for the petals. This design has derives from the AstroMesh reflector antenna developed by Northrop Grumman Astro Aerospace (NGAS), but the opposed geodesic dome structures that normally form AstroMesh antenna surfaces have been removed. They are replaced by tensioned cords or spokes that are loosely fitted with an optically opaque blanket. The spoked structure is actually simpler and can be tuned for better stability of the rim, which is not as important for the domes when forming RF antenna surfaces.

The petals are arrayed around the circumference of the truss with only three kinematic (statically determinate) interface points; two at the base and one provided by a deployable outrigger strut. The petals employ a highly mass efficient lattice structure comprised of pultruded graphite fiber reinforced plastic (GFRP) rods that have finely tuned CTEs to limit thermal deformations. The lattice structure is configured and optimized to provide stiffness and stability as required to meet petal stability requirements. All deployments are passive using stowed strain energy for actuation, dampers for rate control and separately commanded release devices for sequencing.

The thermo-optical micrometeoroid shield (TOMS) is the final major starshade component. The TOMS is a specialized blanketing system that ensures the required optical obscuration, controls petal and truss thermal responses and provides an adequate level of protection from micrometeoroid perforations to keep sunlight bleed-through to an acceptable level for the duration of the mission. It is placed on the side of the starshade facing the telescope and must be compatible with the petal stowage configuration

A full-scale 7.5m long proof of concept (POC) model of a single petal structure is now in production at JPL and will be used to first demonstrate stowage and deployment of the petal structure, then as a test-bed for developing other elements, such as the TOMS, deployment kinematics, petal and outrigger strut interfaces to the perimeter truss. Additional plans are proposed to develop breadboard and prototype hardware of increasing fidelity that will be used to verify the most critical tolerance requirements. This program is intended to develop the starshade to a point suitable for flight project development.

Following a discussion of some key requirements, the starshade system level and petal designs are detailed, preliminary analyses are presented and the plans for developing the starshade technology are discussed.

2. KEY PERFORMANCE REQUIREMENTS

2.1 Mass and volume

A key functional requirement is to be sufficiently lightweight and compact in stowed volume to allow a combined launch of the occulting spacecraft (S/C) with a 1 to 2m-class telescope using an existing launch vehicle (LV). Applicable launch vehicles are the Atlas V and Delta-IV, both with 5m fairings that provide a usable payload envelope diameter of about 4.5m. There are numerous options for launch mass capacity within these vehicle families. Mission studies have developed conservative mass allocations for the two required spacecraft that, in combination with intermediate level LV throw capacities lead to a starshade mass allocation of 1,000 kg. Removing reasonable allocations for the deployable truss structure, central disc and a central hub structure leaves 700 kg for the petals, which corresponds to a generous areal density of over 2.6 kg/m².

2.2 Stiffness

The first natural frequency of the occulter system (starshade and spacecraft bus) must be greater than 0.2 Hz, to avoid adverse interactions with the spacecraft attitude control system. Also, the first natural frequency of individual petals, assuming a fixed base at their truss interfaces, is required to be greater than about 1 Hz to avoid coupling with occulter system modes. In practice, petal stiffness is actually driven by ground handling considerations. It is highly desirable for gravity sag strains to be a small fraction of any component elastic limit so that sag is limited to less than 1.5 cm. This can be achieved with very few gravity compensation fixture (GCF) offload interface points if sufficient petal stiffness is provided. It is highly desirable to minimize the number of required offload points and to locate them conveniently so that it will be possible to fully and autonomously deploy the entire starshade during ground validation and to be able to measure their alignment using advanced photogrammetry techniques.

2.3 Figure control requirements

The establishment of quantitative starshade figure control requirements is a central activity currently underway in the subject development program. The top-level performance requirement is to suppress starlight by a factor of 10^{12} with the nominal petal edge profile. Starshade profile tolerances are allocated to allow a total degradation in the suppression by a factor of 100, which is consistent with the detection of earth-like planets at a contrast level of $4E-11$. Representative tolerance specifications are detailed in Shaklan⁴ (this conference) and Table 1 here summarizes the most critical of these specifications.

Table 1: Critical Tolerance Allocations		
Petal Perturbations	1-sigma Mean error over all Petals	3-sigma Error-over each Petal
Radial position	0.2 mm	1.0 mm
Lateral position	1 mm	0.5 mm
Proportional width	2.0 E-5	7.5 E-5
Profile ripple amplitude*	3 μ m	30 μm
<i>* For sine-waves between 2-12 cycles along petal length</i>		

The optics will tolerate relatively large proportional width, random and large-scale geometric errors in petal edge profile and the petal positional tolerance is feasible. The 1-sigma mean “profile ripple amplitude” of $3\mu\text{m}$ in Table 1, however, indicates that the optical system is highly sensitive to a small range of minute periodic deformations of all the petals simultaneously. We currently know of no structural cause that would result in such an effect, particularly on such a globally consistent scale. Nonetheless, the amplitude of this deleterious deformity falls well within the peak structural deformations that we expect to see on-orbit, which is a concern. This modality of deformation may be more the result of the current mathematical construct used to evaluate error sensitivities than it is a real threat from a structural point of view. Such periodic deformations are likely to be statistically rare as a result of manufacturing errors and avoidable as a result of environmental or other effects by employing design strategies that will mitigate them. This may include attention to geometry, material development and optimization and even grading of components during manufacture. But we must be able to confirm this with our development program.

The suballocation of structural deformations from different sources will not be resolved until physical models of significant petal components can be carefully measured in relevant environments. We need to measure the capability of some unique and new manufacturing methods and explore the extent to which GFRP material properties can be optimized in the novel configurations that are proposed. We need a customized metrology system to conveniently measure as-built and deformed petal edge profiles to the required resolution in the lab. Finally, we will need to complete a significant body of structural analysis using known statistical variations in the constitutive properties of the key components of the petals and the perimeter truss. This is planned as a part of our development effort at JPL.

For now, our understanding of petal-level tolerance requirements and performance is the best developed, so this paper will concentrate on those. Petal position tolerances drive the perimeter truss deployment accuracy and stability. Proportional width tolerances drive the petal manufacturing accuracy and allowable thermal deformations. Petal profile ripple tolerances drive the petal manufacturing measurement and verification methods. An adjustment strategy is planned for fine-tuning the optical edge during integration and if required a new process akin to mirror polishing but with relaxed tolerances and in only two dimensions (a planar curve) will be implemented.

Sun angles relative to the occulter normal axis are kept between 30° and 85° , the former being a telescope limit so that no sun enters the sugar-scoop shaped sunshade baffle. The latter value is an estimated limit required to accommodate combined occulter and starshade pointing and alignment errors while keeping sun off any telescope-facing starshade surface. For most operating cases we expect to limit the latter angle to 70° to control thermal extremes in the starshade components. We know that performance will begin to degrade beyond 70° sun angle to normal in current worst-case predictions, but it is not yet known how significant this degradation will be to mission goals.

Spinning the occulter appears to be a very attractive option as it greatly relaxes the tolerance requirements applied to each petal as the effect of local perturbations is smoothed out over long integration periods, relative to the spin period. This effect is not reflected in Table 1.

Many other detailed and sub-allocated requirements are being compiled and continue to emerge, such as optical edge maximum radius and optical properties, detailed TOMS requirements, station keeping and pointing etc. Nonetheless, the feasibility of the required total mass, stowed volume, figure error and stability are the focus of our efforts at this time.

3. SYSTEM CONFIGURATION

The left view of Figure 2 shows the stowed occulter spacecraft system fitting in an Atlas V 5m fairing of medium height (not the tallest) atop a 1.1m telescope spacecraft system. Dual spacecraft observatory configurations with a 2m telescope still show with margin using an available extended length Atlas V fairing. The starshade stows around a fixed, lightweight central hub structure. Since the petals wrap around the hub to stow, its radius is a key petal design requirement. The hub is sized to provide sufficient annular radius between its OD and the fairing ID to contain the stowed starshade truss and petals while maximizing hub diameter to reduce petal strain. For the 30m O₃ design the hub can be about 3m in diameter. The petals wrap around the hub about 270° circumferentially and overlap about 2/3 of the total stowed truss height vertically. The remaining 1/3 of the stowed truss is visible in the center view of Figure 2. It is estimated that there is sufficient margin to stow a starshade with 50-60m diameter while still reserving sufficient volume for the occulter spacecraft bus systems.

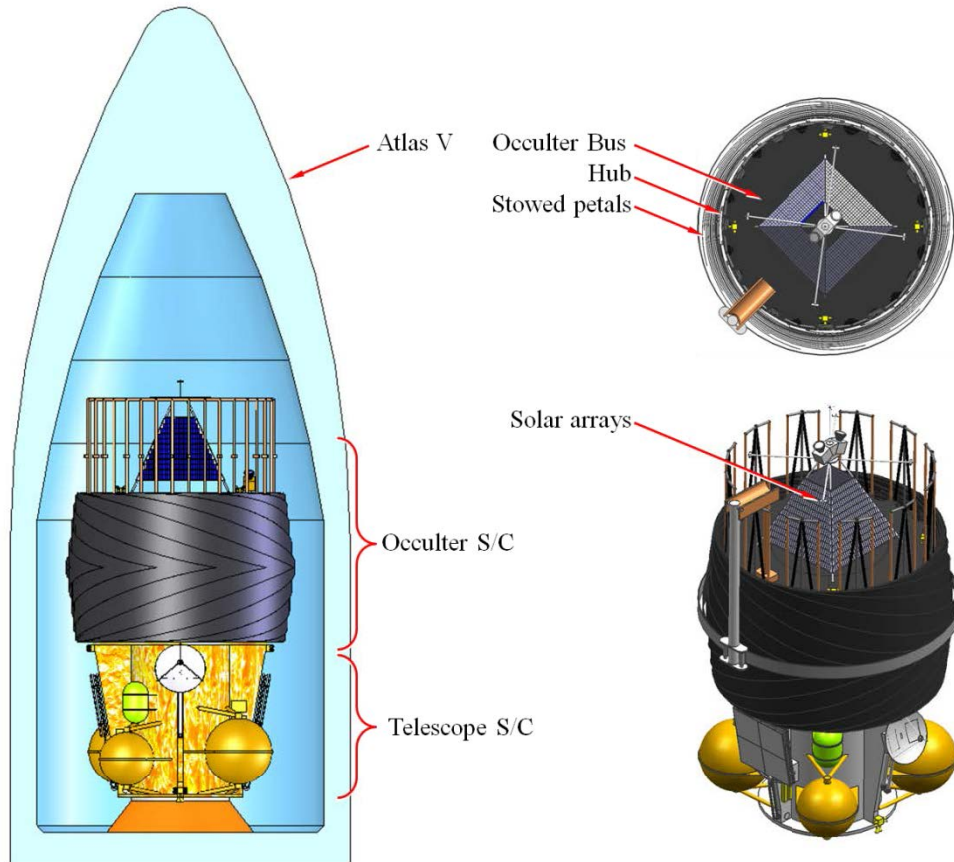


Figure 2. O₃ 1.1m Occulting Observatory stowed in an ATLAS V; Stowed Occulter spacecraft, iso and top views

Bus equipment mounts inside this central hub with protrusions for solar arrays, attitude sensors, thrusters, etc. Fixed solar arrays, configured in a pyramid fashion provide the modest power demand, while limiting the shadows cast by the sun onto the petals. For O₃ the telescope performs the retargeting maneuvers and the propulsion required on the occulter is limited. However, there is ample spare volume inside the central hub to add the propulsion capability for retargeting with the occulter for mission options that cannot have the telescope perform these maneuvers. The O₃ mission can be performed with conventional chemical propulsion, but missions like JWST, with larger separation distances require adopting higher efficiency arcjet thrusters. These thrusters still burn conventional propellant (hydrazine under low pressure) but require more power and therefore larger deployable solar array. The solar array can be deployed in a manner that minimize shadowing of petals.

The perimeter truss, shown in Figure 3, is a very stiff, precise and stable deployed structure and this has been verified by numerous ground tests performed by NGAS Astro and by the results of on-orbit operations of over seven large antennas

flown to-date, of which several were of the same scale as the O₃ truss. This truss design will be modified for the starshade application by the use of stiff, pre-tensioned spokes across the interior instead of reflector dome structures. This will further enhance the precision and stability of the deployed truss rim. The truss rim nodes are in turn the stiff interface points from which the petals are cantilevered, with additional support provided by a deployable outrigger strut for each petal. Each petal is precisely located in-plane to maintain the global figure profile by two latches, one at each corner of the petal root. The latches provide kinematic restraint of the petal in all degrees of freedom except rotation about the axis of the truss longeron adjacent to the root of the petal. This cantilever mode of motion is restrained by the deployable outrigger strut so the flat petal bodies remain aligned with the starshade plane. The result is that the petal/outrigger combination emulates a stiff tripod for structural efficiency. This is essential for achieving a low-mass structural system with high precision.

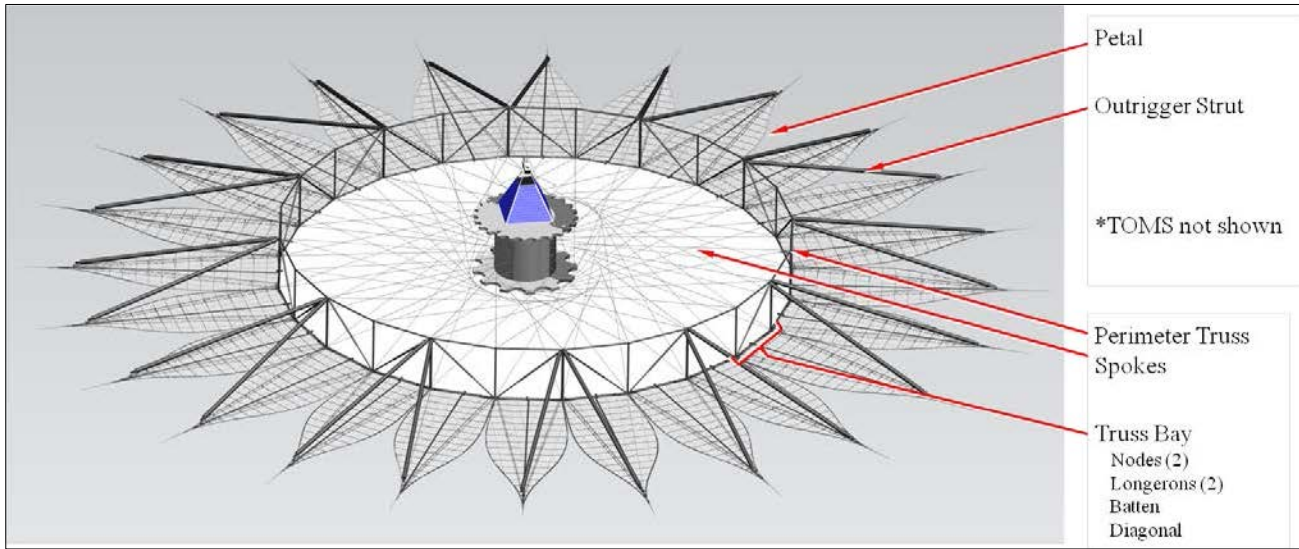


Figure 3 Deployed Starshade

Figure 4 shows unfurling of the petals, the first phase of the deployment sequence. Deployment during this phase is entirely passive through the controlled release of stored strain energy. Unfurling is initiated by release of a belly-band restraint system around the circumference of the stowed starshade (also shown in Figure 2). Lanyards that pay out from spools on passive rotary dampers and/or sequenced release devices such as pyros will meter the rate of unfurling. Once the petals are nearly straight a pair of spring-loaded ribs pops open towards the sun-facing side of the petal to stiffen it and maintain flatness upon deployment. Deployment of the outrigger struts is concurrent with petal unfurling and is also achieved passively. Outrigger concept down-selection is underway now and prototyping commences in FY11.



Figure 4. Deployment phase 1: Petal unfurling

Figure 5 shows perimeter truss deployment, the second and final phase. Truss deployment is accomplished by reeling in a deployment cable on a motor-actuated spool. The cable runs around the circumference of the truss inside the telescoping diagonal members, which are extended when stowed. Spooling in the cable forces the diagonals to retract, which deploys the truss. Each bay of the truss is synchronized to its neighbor by synchronizer gear pairs that are attached to adjacent longerons at every other truss node. The petals simply follow the truss as it deploys to complete their 90° rotation into the plane of the starshade. When truss deployment is nearly complete all petal root latch pairs engage and latch to the truss nodes. The outrigger struts also latch in place, either passively or by commanding a single latch release device ganged to all outrigger latches via a cable.

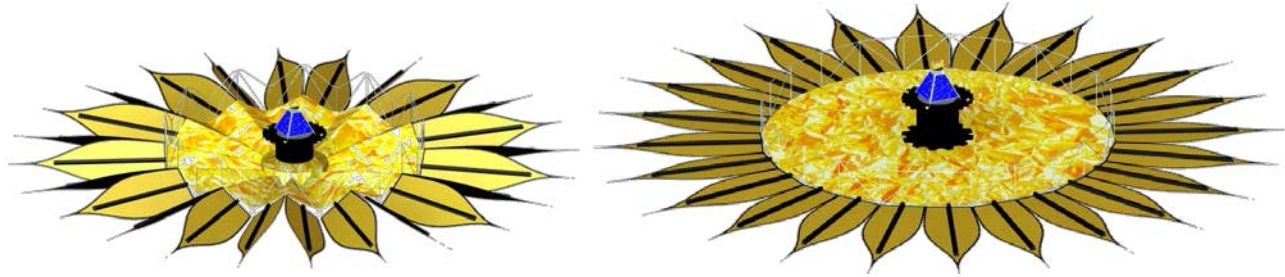


Figure 5. Deployment phase 2: Truss deployment

In summary, the starshade takes advantage of the kinematics of the deployable perimeter truss, which in itself is highly mass and volumetrically efficient, as a base and prime mover to deploy an extremely large, precise and stable deployable structure with an economy of actuators and kinematic steps. The structural context of the truss allows the petals to be very lightweight without needing much parasitic structural mass to support them for launch. It also provides stiff structural interfaces close to the petal roots for high deployed petal stiffness with minimum mass, as we will see in the following paragraphs.

4. PETAL DESIGN

Figure 6 details the petal structural design, as viewed from the telescope (anti-sun) side, with the TOMS blanket removed. The primary petal structure is a lattice of battens and longerons that intersect a longitudinal spine and a pair of structural edges on each side. These elements are optimized to place and precisely maintain the optical edge with the required profile tolerance regardless of thermal extremes or structural loads from the relatively thermally unstable TOMS. The lattice is highly mass efficient yet very stiff in-plane. Secondary petal structure includes a pair of deployable ribs in an “A” frame configuration that stiffen and maintain overall deployed petal flatness. The deployable ribs fold outward and flat against the petal when stowed then pop up into place when the petal is unfurling. The ribs are deployed by extension springs that are inside hollow soda-straw size GFRP struts that lock the ribs in place at a near-perpendicular angle to the petal when deployed. The ends of the deployable ribs coincide with truss-to-petal interface nodes on the base spine and with the outboard end of the outrigger at the apex of the “A” to complete the tripod-like geometry of the petal and outrigger support structure on the edge of the perimeter truss. The driver for sizing the ribs and battens is actually a 1-g petal gravity-sag displacement requirement of <1.5 cm with the TOMS installed. This insures that a truss and petal alignment verification can be performed on the deployed starshade with high confidence prior to launch.

The battens define and maintain the precise petal edge-to-edge width. They are made from a pultruded GFRP base material that has a room-temperature axial CTE of better than $-0.2E-6/C$. It is not well known in aerospace circles that this inexpensive material can be made with near-ideal and highly consistent uni-directional fiber volume content, which gives it excellent properties for our purpose. It can also be pultruded in almost any required cross-sectional shape. The battens are continuous across the width of the petal so that joints will not affect their axial stability. To maintain edge profile tolerances the CTE of the batten base material will be nominally zeroed-out using one or more of several proven strategies that will be selected during the planned development program. We believe that petal profile tolerance requirements can be met with: 1) a nominal CTE of zero at room temperature, 2) temperature dependent CTE variation of less than $0.2 E-6/C$ and 3) CTE scatter and structural hysteresis less than $\pm 0.1E-6/C$. Ultra-high modulus material is not required, so this level of performance should be achievable. Our development plans include a comprehensive material development effort to achieve and verify this level of batten material performance. Finally, batten-to-batten spacing along the petal length is arbitrary, so it will be varied to avoid systematic petal edge profile ripple at sensitive spatial frequencies.

Longerons provide the petal with in-plane shear stiffness for maintenance of the overall shape. They are made from the same pultruded GFRP as the battens, have a circular cross section and are also continuous along their length. The longest pair of longerons also act as hinge pins for the deployable ribs. Like the battens, the number and placement of longerons is somewhat arbitrary. The longitudinal and base spines provide additional stiffness and are constructed of a foam core sandwiched between thin graphite face sheets. The base spine closes out the petal root structure and carries the perimeter truss interfaces: two hinge points for the unfurling portion of deployment and two precise latches that position the deployed petal in-plane.

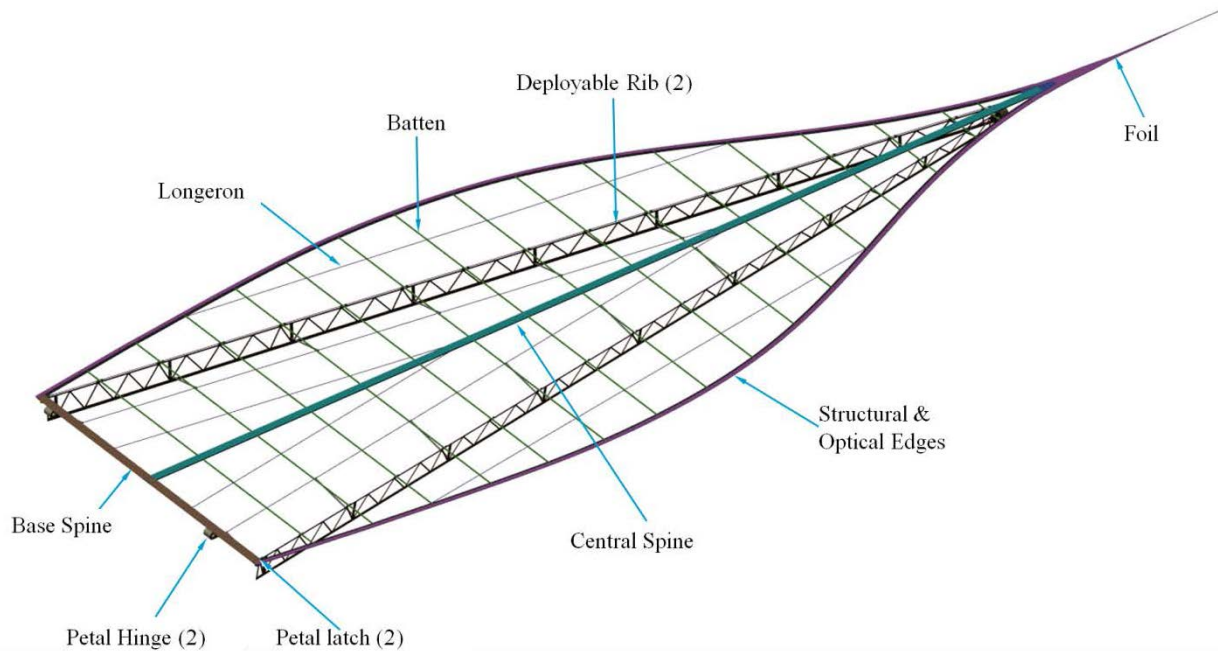


Figure 6. Petal design details

All petal structures are designed so that no component is subjected to more than 0.5% strain (5000 μ strain) when stowed around the 3m diameter hub. This design constraint insures that significant permanent set or creep that would degrade the deployed shape or figure of the starshade will not occur. This level of strain is only approached by the longitudinal spine in our current design, which has little or no role in the definition of the deployed petal edge profile. It's primary function is to accommodate launch restraints and deployment hardware and as a ground-handling interface. The battens are perpendicular to the direction of stowed petal strain and thus will not experience permanent set from material creep prior to launch.

The structural edge defines the perimeter of the petal structure and is made of high-modulus quasi-isotropic GFRP laminate of 3mm thickness and sufficient width to provide stability in the petal width direction between batten tips. The optical edge system is attached to the structural edges and is comprised of two types of components: 1) GFRP strips made of laminate identical to the structural edges but only 0.5mm thick and which extend slightly beyond the structural edges to define the optical petal profile and 2) a slender 2.5m long foil with a widened base that attaches where the structural edges converge to a point. The foil is approximately 2mm wide over most of its length. The optical edges are beveled to minimize the forward scattering of light toward the telescope and are finished with the required radius. The optical edge strips are made in replaceable segments and can be absent during large portions of the integration and test program to avoid damage and even permit modest optical profile changes late in the integration flow. The optical edge strips are fastened to the structural edge periodically with simple mechanisms that can be adjusted laterally through a range of $\pm 50\mu\text{m}$ with a resolution of approximately $2\mu\text{m}$ or better. Detailing and testing the optical edge scatter performance is the subject of a separate technology effort, funded by a NASA TDEM and executed by Lockheed-Sunnyvale and Ames Research Center.

The production strategy for establishing the figure profile is to first fabricate the petal structure with conventional precision composite fabrication techniques. This will yield a tolerance of better than $250\mu\text{m}$ for the periodically spaced holes in the structural edge that interface with the optical edge components. The resulting location of these interface holes will then be measured to within $1\mu\text{m}$ or better using a customized laser metrology system mounted on a large optical bench with the petal. These measurements will determine the dimensions that will be machined into each the optical edge component for a matched fit based on its location in the petal. This step requires higher manufacturing precision more easily achieved on the small scale of the optical edge segments than the full petal structure. The optical edge profile is re-measured after integration with the petal structure and tuned as necessary with the mechanical adjustment features and a polishing procedure, if necessary. Initial petal measurement, optical edge integration and profile verification take place with the petal restrained out-of-plane on the optical bench fitted with $1\mu\text{m}$ accuracy

metrology system. Lower resolution photogrammetry data for each petal will also be used before the optical edges are match-machined and integrated with the petal. This data will be processed from as-built deployed petal shape measurements made during deployment testing done prior to edge integration. All gravity effects will be removed using a validated structural FEM developed so that the as-built zero-gravity petal shape can be known. With this data any foreshortening of petal profile dimensions due to petal out-of-flatness can be removed by accounting for it during fabrication of the optical edge.

The thermo-optical micrometeoroid shield, or TOMS (not shown in Figure 6), is a multi-functional blanket assembly that mounts on the telescope-facing side of the petal structure. It presents an opaque, optically black surface to the telescope and provides thermal control for the petal and truss central disc. The TOMS also functions mechanically to mitigate the effect of micrometeoroid perforations, act as a buffer between the stowed petals and help to damp out launch vibration. The TOMS is vented for launch ascent and is loosely attached to the petal structure with insignificant structural coupling. The baseline blanket concept consists of a non-woven fibrous felt sandwiched between 2 layers of black Kapton.

Thermal properties of the TOMS are selected to minimize on-orbit temperature excursions of the petal and truss structures and to center nominal petal operating temperatures close to room temperature, at which they were fabricated. The black high emittance surface facing the sun serves to apply a near-uniform heat load to both sides of the petal structure. The felt serves to space the Kapton layers, such that the plasma created by small micrometeoroids striking the first Kapton layer is dissipated prior to striking the second layer. The felt may also contribute to dissipating the plasma and may provide a level of self-healing due to the elastic nature of the fibers. Most of the particles that are large enough to pass through both layers of Kapton will be on trajectories that do not line up with the telescope, so sunlight passing through them will not degrade occulting performance. Light that does pass through both holes may be attenuated by the felt fibers.

The petal areal mass estimate for the current petal design is probably conservative in some areas of its design. It is still based on a number of non-optimized initial sizing estimates and on the mass of certain components and materials that happen to be available for low-cost proof-of-concept and breadboard models. Nonetheless structural performance goals are well in-line with requirements and the current best estimate (CBE) for petal areal density is 1.5 kg/m^2 . This is compared to the 2.6 kg/m^2 allocation or a contingency of 73% on the allocation.

5. ANALYSIS RESULTS

5.1 Structural analysis

Structural analysis started with detailed modeling of an individual starshade petal and progressed to a preliminary full occulter system-level model including petals, perimeter truss, spokes, hub and spacecraft. Petal stiffness was driven by a 1G deployed deflection requirement of 1.5 cm (including offloading) with the goal of approximately 1 cm. As such, a deployed petal with rigid boundary stiffness at its three interface points has a first mode frequency of approximately 3Hz. For the full system we had a minimum first mode frequency requirement of 0.2Hz and a goal of 0.5Hz which was achieved.

Occulter petal model

The baseline “herringbone” petal model is composed of detailed representations of all components except for the TOMS, which is modeled as a distributed mass (approximately $\frac{1}{2}$ the total petal mass) and for the optical edges that are on each side of the petal since they will be kinematically decoupled from or insignificant to the large-scale structural behavior of the petal. The tip foil, however, is modeled.

NASTRAN is being used for most of the Finite Element Modeling (FEM) work. ABAQUS has also been used for some of the large-deflection nonlinear petal component deployment analysis. Petal components are modeled using a combination of plate, solid and beam elements with composite properties as appropriate. All degrees of freedom for mechanical details of the structure are also modeled, such as in the rib hinges, which are equivalent to somewhat loose and sparsely pinned piano-hinges.

Figure 7 shows the 7.5m long O₃ petal FEM which has 848 nodes and 1190 elements. Figure 8 shows a plot of the petal normal mode frequencies and modal effective mass fractions for the petal constrained at 3 points as indicated in Figure 7. Figure 9 shows a plot of the mode-shape (arbitrary amplitude) for the 1st mode at 3.2Hz. Since optical performance of

the occulter is most affected by in-plane motion of the petal, modes with large effective mass in the X and Y directions would indicate significance. Such a mode is not seen until well over 5 Hz.

The 1G deflection of the deployed petal is important for the facilitation of ground performance verification. Our goal was to have a maximum displacement of approximately 1cm for the petal in 1G while using off-loading supports. Figure 10 shows the resulting displaced shape (scaled) and displacement contours, for the case of using 6 support points: two at the base, one near the rib-rib intersection and three more intermediate points (center-spine and two edges). We get a maximum displacement of around 1.16m for this case, which is acceptably close to our goal of 1 cm.

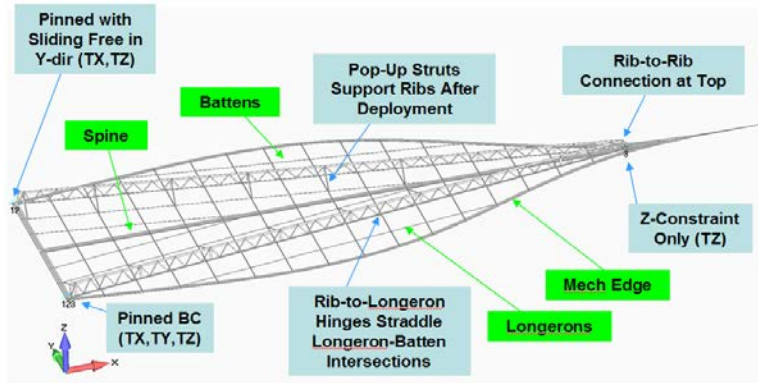


Figure 7. Petal FEM Description

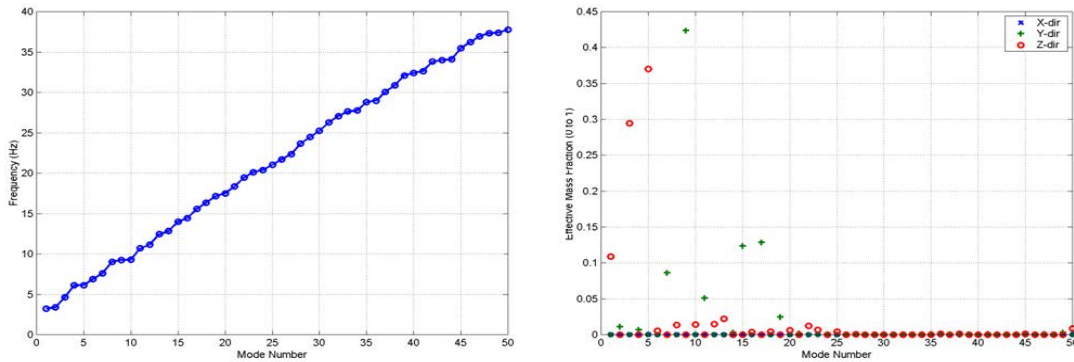


Figure 8. Petal FEM normal mode frequencies and effective mass fraction

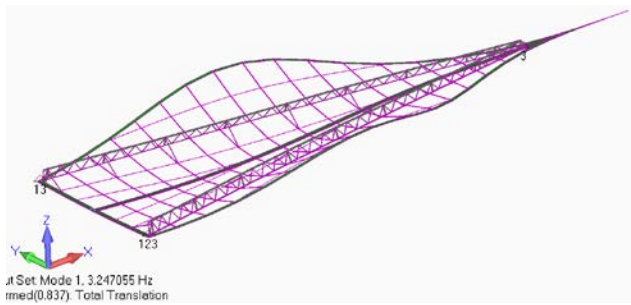


Figure 9. Petal 1st mode (3.2Hz) mode-shape

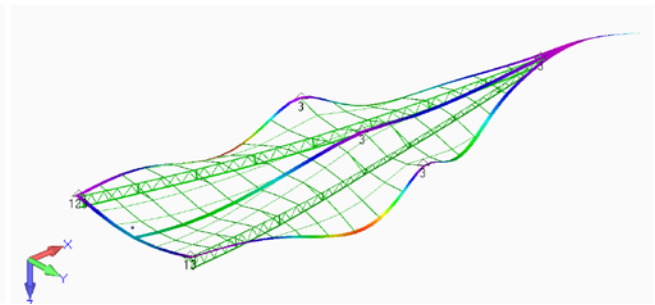


Figure 10. Off-loaded petal 1G displaced shape and contours (T3)

Occulter system model

The O₃ Occulter system FEM given in Figure 11 was created by duplicating the detailed petal component model 24 times and attaching them with representative fitting elements to a perimeter-truss. Outrigger-struts connect the other end of the perimeter-truss to the petals at points near their rib-rib intersections. Pre-tensioned cables are used as spokes connecting the hub and occulter spacecraft bus to the perimeter-truss. The analysis results shown below do not include geometric/differential stiffening effects of the cables, which will be analyzed using NASTRAN's nonlinear analysis.

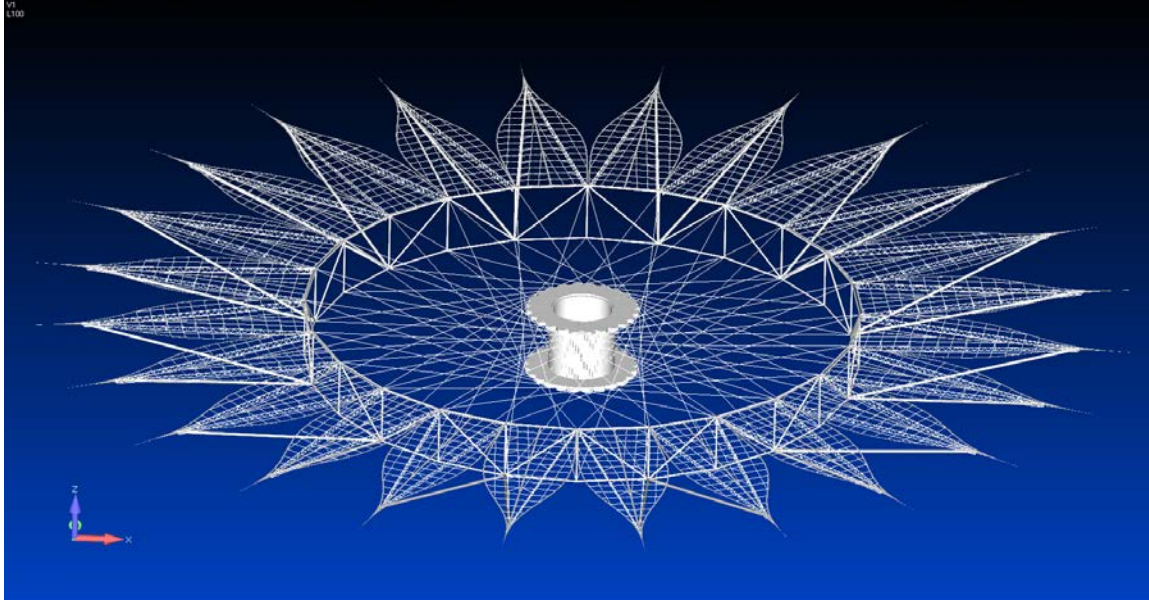


Figure 11. O₃ Occulter system FEM

Figure 12 shows the O₃ Occulter normal mode frequencies and mode-shapes for the first 12 elastic modes. The 1st mode frequency is 0.52Hz which meets our goal of 0.5Hz. We can see from the mode-shapes that the petals act as rigid bodies on the edge of the more flexible truss for these first 12 elastic modes since they are below the first petal mode of 3.2 Hz.

The system modes display a similarity to Zernike circular polynomials. The mode-shapes of modes 7 & 8 (the 1st two elastic modes) are analogous to astigmatism, modes 9 & 10 to trefoil, modes 11 & 12 to quadrafoil, modes 13 & 14 to pentafoil and mode 15 to hexafoil. Mode 16 is a plunge mode analogous to power and modes 17 & 18 are analogous to coma. It should be noted that even though these mode-shapes are dominated by out-of-plane motions of the petals, the actual modal response levels were quite small for the transient excitation analyses studied.

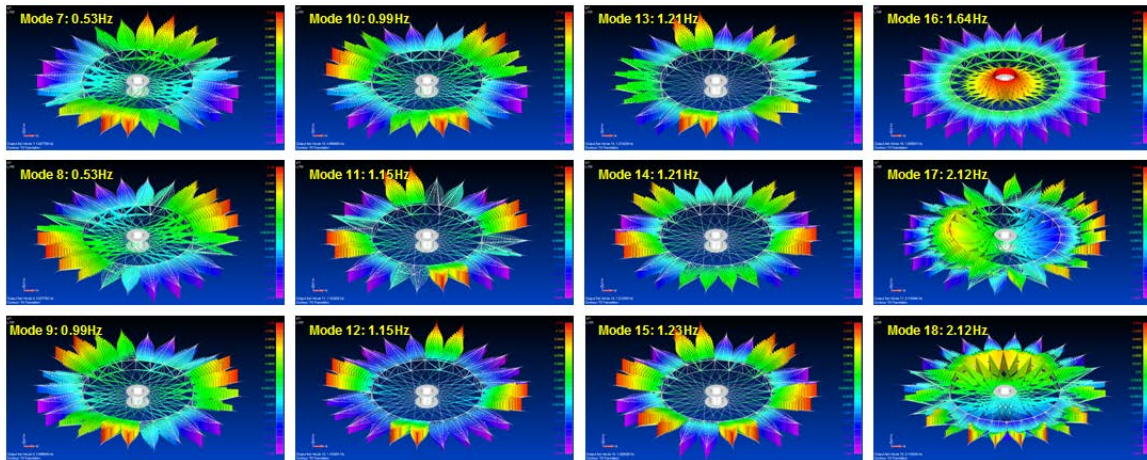


Figure 12. O₃ Occulter System normal mode frequencies and shapes

Some mission options require the occulter spacecraft to maintain alignment with the telescope line of sight by providing lateral station keeping. We have evaluated the dynamic response to firing thrusters for this purpose. Figure 13 shows occulter transient response to thruster pulses of 1N for 8s and 4N for 2s respectively. Uniform modal damping of 1% was used for these analyses and experience indicates this is a reasonable guess until damping can be evaluated.

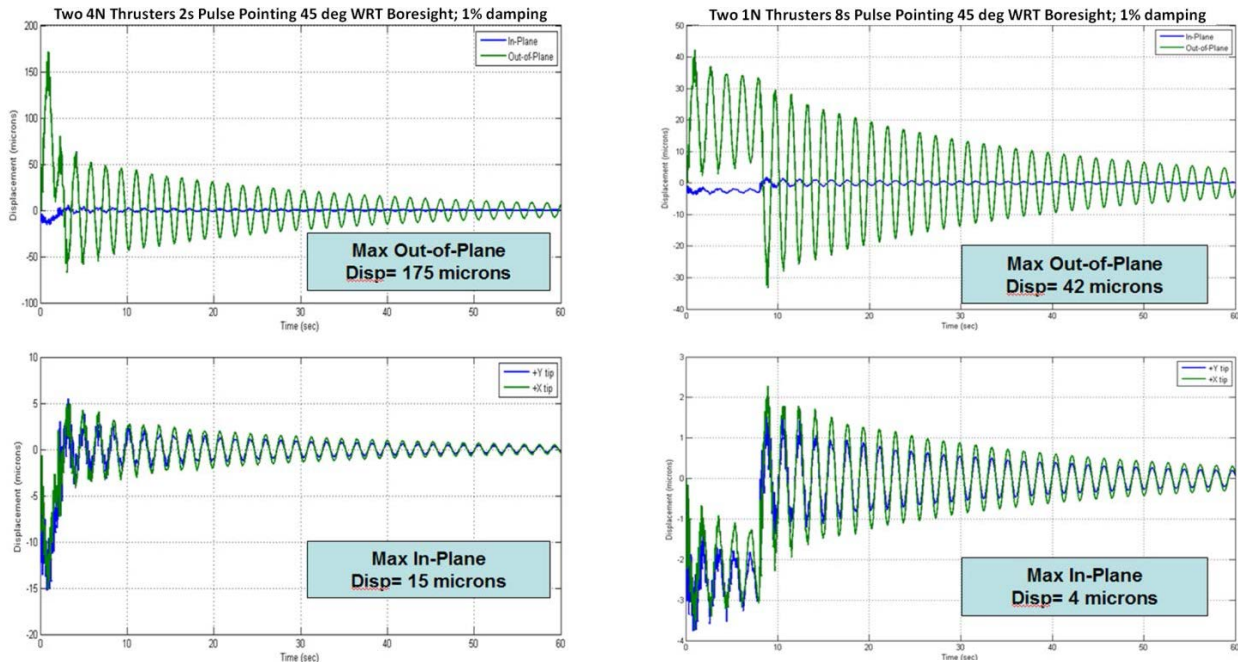


Figure 13. Occulter system responses to nominal thruster firing

The resulting in plane perturbations are limited to about 15µm and this damps out within about 30 seconds. We have also studied the effect of scaling the occulter up by a factor of 2. The first mode dropped by an inverse ratio, but was restored over 0.5Hz by simply doubling the spoke stiffness.

5.2 Thermal Analysis

The occulter system, including spacecraft, was thermally modeled using IDEAS-TMG. The model is very detailed for one petal and simplified for the other 23 petals, perimeter truss and spacecraft as shown in figure 14. Spacecraft, perimeter truss and local petal geometries are critical for capturing shadowing effects and are modeled.

The key thermal issue for petal deformation is the deviation of batten temperatures from room temperature as sun angles change during and between science observations. Thermal strains in the battens are the primary source of on-orbit petal profile errors. With a batten CTE of $-0.2E-6/C$ (potential range and variations discussed above) and the specification of

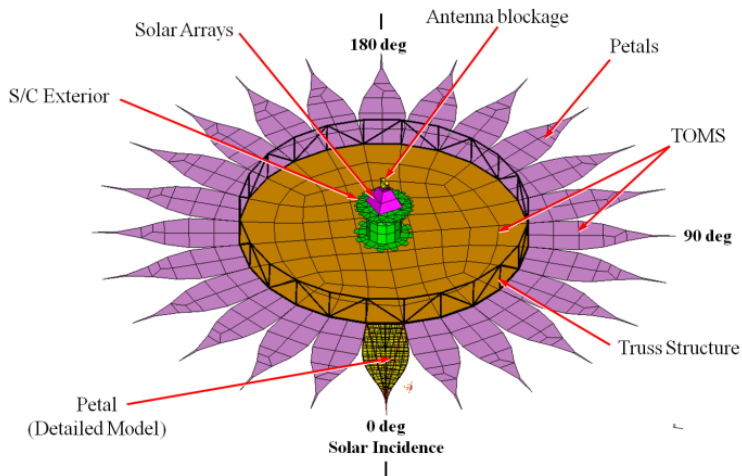


Figure 15. Occulter thermal model

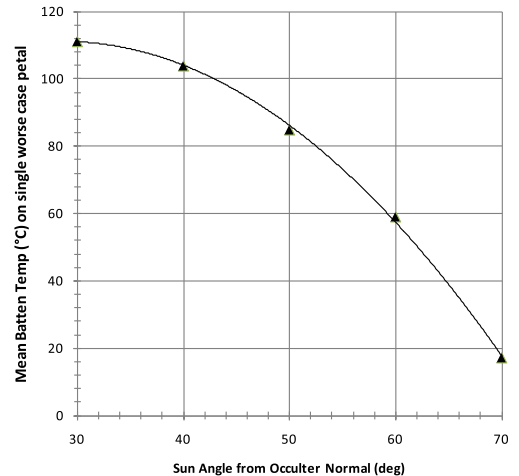


Figure 14. Average batten temperatures vs. sun angle

2.0E-5 1-sigma proportional width error, an average temperature excursion of 100C for all petals simultaneously would consume the entire deformation budget. Figure 15 shows the worst-case predicted average batten temperature as a function of sun angle for battens at the petal base (about 2m wide), mid-point (about 2.5m wide) and approaching the foil (1m wide). The worst case occurs when a petal is azimuthally oriented 180° from the Sun and sun elevation angles are over 70° (defined relative to the telescope line of sight) so that spacecraft shadows fall on that petal. The change from room temperature is 100C for sun angles between 30° and 70°. In this case our design strategy would be to bias the shape of the petal during fabrication so that the correct nominal optical width is achieved at room temperature plus 50C and retain 50% of the 1-sigma proportional width error allowance for other error sources. At sun angles greater than about 75° batten temperatures drop precipitously and will exceed our strategically adjusted allocation of +/- 50C for temperature change. There are a number of potential mitigating factors, however: 1) the 1-sigma tolerance is defined for all petals simultaneously and the 3-sigma requirement may afford significant headroom; 2) placing the spacecraft shadow in-between petals can temper the worst-case and 3) spinning the occulter relaxes requirements by smearing deformations over time and it may help to damp thermal response of the starshade. The overall effect on performance is under continuing study; in the event that a sun elevation constraint of less than 85° is required, design reference mission (DRM) study has shown that this does not have a large impact on science goals.

6. DEVELOPMENT PLAN

A full-scale proof of concept model of a single petal is currently in development at JPL and scheduled for completion by October 2010. This model will be used to demonstrate the first stage of deployment (petal unfurling only), validate the structural model with measurements of gravity sag and modal testing and finally as a testbed for developing other parts of the deployment system. Plans are in place to follow-up this effort with the development of breadboard and prototype petals of increasing fidelity with a flight-like design over the next two years. These models will be used to demonstrate figure and deployment tolerance capabilities and figure stability including during and after thermal cycle testing. A demonstration of figure stability constrains the need for precise figure measurements to a flat optical bench rather than in the deployed configuration. An additional model of a representative portion of the petal is planned and sized to fit in existing T/V chambers for precision CTE characterization and to verify the structural modeling of thermal deformations.

The overall objective of this early (pre-project) development plan is to raise the technology readiness of the starshade to TRL 5 by focusing on novel aspects of the system such as the petals and outriggers for intensive technology development activity while relying upon the heritage of other components such as the perimeter truss.

7. CONCLUSIONS

There are several technological challenges to be overcome for us to be ready to fly an exoplanet occulting mission. The one foremost on the minds of mission planners may be the feasibility and affordability of the large deployable starshade that is required. In this paper we have shared a starshade preliminary design that appears mechanically feasible through the use of heritage deployable structure designs and the reasonable application of state-of-the-art composite and mechanical components in an evolutionary context. There are still a number of typical deployable structures developmental challenges ahead such as the detailed nature of launch restraints and deployment rate-control mechanisms, but these look entirely feasible with the primary challenge being to keep complexity low. Predicted petal mass is about 1.5 kg/m² versus an allocation of 2.6 kg/m² which places the total starshade CBE mass at about 530kg versus the allocation of 1000kg. Stowed volumetric performance of the design should allow an occulting observatory consisting of a telescope up to 2m diameter to be dual-launched with an occulter of 50-60m diameter in currently available launch vehicles. This deployable structure will certainly offer unique developmental struggles due to its sheer size, complexity and validation needs such as in ground testing, metrology, manufacturing methods and facilities costs. Fortunately these challenges are no more daunting in scope than those that have already been overcome for the making of mesh reflectors and large-scale optical instruments, possibly even less so in many areas.

Nothing has yet flown or been demonstrated on the ground that does what we will require of the starshade. Heritage large mesh reflectors of similar scale that continue to be flown must deliver precision to somewhat less stringent values than the starshade, with RMS surface figures of 8E-5 being the approximate on-orbit state-of-the-art and 3E-5 near the probable limit for passive control of mesh reflector shape using the heritage approaches. Although starshade and mesh reflector geometric precision specifications are not directly comparable, they are compared in Table 2 to give us a sense of scale. Note that mesh reflectors must deliver 3-dimensional surface figure tolerances, not 2-dimensional edge profile performance. It is reassuring when one considers that it is far easier to design a structure to deliver any given in-plane

profile tolerance than it is to provide a comparable doubly-curved surface figure tolerance. The table shows that starshade petal radial and lateral position and proportional width tolerances fall into the same range as 3-D mesh reflector capabilities. Aside from anything that we have predicted in this study, Table 2 should be quite reassuring.

Table 2: Critical Tolerance Comparison with Mesh Reflectors			
Mesh Reflector Surface RMS/diameter: 8E-5 to 3E-5		Starshade	
		1-sigma Mean error over all Petals	3-sigma Error- over each Petal
Radial position	N/A	6.7E-06	3.3E-05
Lateral position	N/A	3.3E-05	1.7E-05
Proportional width	N/A	2.0 E-5	7.5 E-5
Profile ripple amplitude*	N/A	1.0E-07	1.0E-06

** For sine-waves between 2-12 cycles along petal length*

Nonetheless the most demanding starshade profile tolerance appears to be 1-2 orders of magnitude smaller than what we are comfortable with when considering sensitivity to the amplitude of profile errors with periodic spectral content of 2-12 cycles per petal. Such deformations will no doubt exist well within the amplitude of systematic and random errors that will be machined and thermally induced in the starshade. To what extent these errors propagate and can be controlled is a core subject of study for work ongoing at JPL. Likewise, understanding sensitivity of the optical system to errors in the context of how they actually occur is another central aspect of our work. This entails continuing integration of thermal, structural and optical models as they are refined and run in Monte Carlo simulations with well defined material constitutive property and manufacturing statistical error bands. This is an iterative process because the requirements will be re-allocated between error sources several times as we understand and improve the structure to achieve not only optimal performance but an optimally sub-allocated requirements set.

To reiterate, our plan to perform measurements on physical models of significant petal components in the relevant environments over the coming months is crucial to verify the feasibility of an occulting mission enabling starshade. We will validate the capability of several unique and new manufacturing methods and explore the extent to which pultruded GFRP material properties can be optimized over wide temperature swings in the novel configurations that are proposed. We will develop a customized metrology system to conveniently measure as-built and deformed petal edge profiles to the required resolution in the lab. Finally, we will need to complete a significant body of structural analysis using known statistical variations in the constitutive properties of the key components of the petals and the perimeter truss. This is all planned as a part of our development effort at JPL.

Acknowledgments

The research described in this (publication or paper) was carried out at the Jet Propulsion Laboratory, California Institute of Technology, under a contract with the National Aeronautics and Space Administration.

REFERENCES

[1] 1. Spergel, D., et al., “THEIA: Telescope for habitable exoplanets and interstellar/intergalactic astronomy,” in [AAS Meeting 213], 458(04), American Astronomical Society (2009).
 [2] Cash, W., et al., “Direct studies of exo-planets with the New Worlds Observer,” in [Proceedings of SPIE], 5899, 58990S (2005).
 [3] Savransky, D., et al., “Occulting Ozone Observatory Science Overview”, SPIE 7731-88 (2010).
 [4] Shaklan, S., et al., “Error budgeting and tolerancing of starshades for exoplanet detection”, SPIE 7731-87 (2010).